PHYSICAL REVIEW B VOLUME 45, NUMBER 12 15 MARCH 1992-II

Electronic properties and multifractality of a one-dimensional hierarchical system in the presence of an electric field

G. Y. Oh, C. S. Ryu, and M. H. Lee
Department of Physics, Seoul National University, Seoul 151-742, Korea
(Received 6 June 1991; revised manuscript received 16 September 1991)

We study the influence of an applied electric field F on the electronic properties of a one-dimensional system with hierarchical potential strengths. By the method of the Poincaré map, we calculate the transmission coefficient T as a function of the system size N. For small fields, it shows an algebraically localized behavior. With increasing field strength, a delocalization of the field-induced localized states occurs and T shows extended behavior for $R<2$ while it retains a power-law localized behavior for $R>2$. We perform a multifractal analysis on the wave functions of the field-induced states and find the multifractal property in the field-induced extended states.

I. INTRODUCTION

The electronic properties of one-dimensional systems in the presence of an external electric field have been a problem of continuing interest in condensed-matter physics. The application of an electric field has been shown to result in distortions of field-free bands and formation of additional states that have interesting properties.

In periodic systems, there has been a controversy about the existence of Wannier-Stark ladders in the presence of an electric field for some time, but their existence is by now well established both theoretically[1,2] and experimentally.[3] The ladder structure consisting of resonance states, in a strict sense, survives only when the interband tunneling, the so-called Zener tunneling, is sufficiently small. For large fields, the electron in a band gains enough energy to tunnel to the neighboring band so that the spectra form a continuum.[4] These facts can be explained well by Zener's tilted band picture. For disordered systems, it is well known that the applied electric field changes exponentially localized states to power-law localized states[5] and leads to a transition from power-law localized states to extended states at some critical field, as has been rigorously proved by Delyon *et al.*[6] Therefore the existence of three different states in the presence of an electric field is by now well established. Note that Wannier-Stark ladder resonances are also found in disordered systems.[7]

On the other hand, the effects of an electric field on systems intermediate between periodic and disordered ones are not well understood. Examples of such intermediate systems are quasiperiodic[8] and incommensurate[9] systems. Several properties of these systems in the absence of an electric field have been established. For instance, quasiperiodic systems with a Fibonaccian array of potentials are known to have Cantor set spectra of zero Lebesgue measure and critical states, while those with generalized Fibonaccian array of potentials[10] can have three different states; localized, critical, and extended states. Incommensurate systems are also known to have three different states, depending on the site energy.

Another important example of intermediate systems arising in diverse physical contexts is a hierarchical system[11–14] that has irregular deterministic potential structures and exhibits unusual features with respect to periodic, quasiperiodic, and disordered cases. Würtz *et al.*[11] studied a one-dimensional tight-binding model with a hierarchical potential strength (diagonal model) using the recursion relations for renormalization-group transformations and for traces of transfer matrices, and elucidated the nature of the energy spectra and the wave functions. Ceccatto, Keirstead, and Huberman[13] and Roman[14] studied similar models with a hierarchical array of hopping-matrix elements (off-diagonal model), and obtained results similar to those of Fibonaccian quasiperiodic systems; i.e., the wave functions are critical, and the energy spectra form a Cantor set. Roman[14] also performed a multifractal analysis on both the energy spectra and the wave functions, and demonstrated multifractal behaviors of both of these quantities. It is by now well known that critical states have multifractal behavior for all length scales, while extended and localized states do not.

But, as far as we know, most of the models studied are tight-binding ones. Furthermore, the effect of an electric field has not been studied to date. These tight-binding models show the underlying physics clearly, but they are nonetheless one-band models and thus do not treat the electronic properties of the system properly when the system undergoes interband transitions in the presence of an electric field. Therefore we consider a continuum model (or a scattering model) that contains multiband information. With this model, we study the effect of an electric field on the one-dimensional hierarchical system.

In Sec. II, we introduce the structure of a model system and methods of calculating the density of states (DOS), transmission coefficient T, and fractal dimension $f(\alpha)$. The results of numerical calculations and discussions are also given in the section. Section III is devoted to a brief summary of the results.

II. METHODS AND RESULTS OF THE CALCULATIONS

We consider a one-dimensional Schrödinger equation

$$\left[-\frac{d^2}{dx^2}+\sum_{n=1}^{N} V_n\delta(x-x_n)-Fx\right]\Psi(x)=E\Psi(x)\ , \tag{1}$$

where the potential strength of the nth site is given by

$$V_n=U_0R^k;\quad n=2^k(2l+1),\quad l\geq 0,\quad k\geq 0\ . \tag{2}$$

Here N is the size of the system, F is the strength of the electric field, k is the level of hierarchy, x_n $(=na)$ is the nth site of the lattice, and we adopt units in which $\hbar^2/2m=1$, $e=1$, and $U_0=1$, with no loss of generality.

In the absence of an electric field, the system has different properties, depending on the magnitude of the hierarchy parameter R. The system is periodic with lattice constant $a=1$ for $R=1$ and with $a=2$ for $R=0$. In these cases, the system has extended states and the spectrum has an absolutely continuous one. However, for general values of R, the system no longer has simple potential values. In these situations, the system is known to have interesting characteristics.

Equation (1) can be transformed into a second-order difference equation between the $(n-1)$th, nth, and $(n+1)$th sites by a ladder approximation that ignores the continuous variation of the linear potential term and adjusts the potential in each cell to the mean value in that region. Since the essential effect of an electric field is to shift the energy of each equivalent potential, the ladder approximation does not alter the essential physics of the problem.[2] Moreover, it allows one to use plane waves instead of Airy functions, and thus leads to relatively easy numerical calculations with considerable algebraic simplifications. In view of these facts, many authors have successfully used this approximation.[5]

Taking the plane-wave solutions to Eq. (1) in each cell, and using the boundary conditions for the continuity of $\Psi(x)$ and the discontinuity of its derivatives at $x=x_n$, one can obtain the following equation, called the Poincaré map representation:

$$X_n\Psi_{n+1}+X_{n-1}\Psi_{n-1}-E_n\Psi_n=0\ . \tag{3}$$

Here

$$E_n=V_n+X_nY_n+X_{n-1}Y_{n-1}\ , \tag{4a}$$

$$X_n=\frac{k_n}{\sin[k_n(x_{n+1}-x_n)]}\ , \tag{4b}$$

$$Y_n=\cos[k_n(x_{n+1}-x_n)]\ , \tag{4c}$$

and $k_n=[E+F(x_n+x_{n+1})/2]^{1/2}$ is the momentum in the nth cell. Equation (3) is formally analogous to the tight-binding model, but it is equivalent to Eq. (1) and contains all the band-structure information. Thus it is an appropriate equation with which to study the effect of an electric field on the system.

A. Density of states

First we calculate the density of states in the absence of an electric field in order to see the global properties of the system. When Eq. (3) is rewritten in matrix form, $(\mathbf{H}-E\mathbf{I})(\Psi)=\mathbf{0}$, the N-dimensional matrix $(\mathbf{H}-E\mathbf{I})$ becomes tridiagonal. Thus we can calculate the distribution of its eigenvalues, i.e., the DOS, using the negative-eigenvalue theorem:[15]

$$D(E)=\frac{1}{N}\frac{\eta(E+\Delta E)-\eta(E)}{\Delta E}\ . \tag{5}$$

Here $\eta(E)=\sum_{i=1}^{N-1}\eta_i(E)$ is the number of negative eigenvalues of the matrix $(\mathbf{H}-E\mathbf{I})$, and $\eta_i(E)$ is zero for $n_i>0$ and is 1 for $n_i<0$ with $n_i=-E_i-X_{i-1}^2/n_{i-1}$ and $n_0=-E_0$.

To confirm the results on the DOS obtained by the negative-eigenvalue theorem, we use the transmission coefficient to be introduced in the next section and calculate the inverse localization length defined by $\gamma=-\ln T/N$. Figure 1 shows the results on γ and the DOS for $R=1.5$ and $N=2^{11}-1=2047$. Two quantities have exactly opposite behaviors; i.e., the DOS vanishes for large γ but it is large for small γ. In the figure, we can see that the main band splits into many subbands. For general values of R, the number of splitting is 2^k-1, resulting in 2^k subbands for a given level of hierarchy k. The R dependence of the DOS is shown in Fig. 2. The spectrum for $R=1$ represents the case of a periodic system. Since the potentials of the system have the same values, the splitting of a band does not occur and the bandwidth remains constant, forming an absolutely continuous spectrum for any level of hierarchy k. However, in the regime $R>1$, the increase of the level clusters the eigenvalues, resulting in highly concentrated spectra. The relative width of allowed bands will go to zero as the level of hierarchy increases. Thus the spectrum in the infinite-system-size limit will form a singular continuous

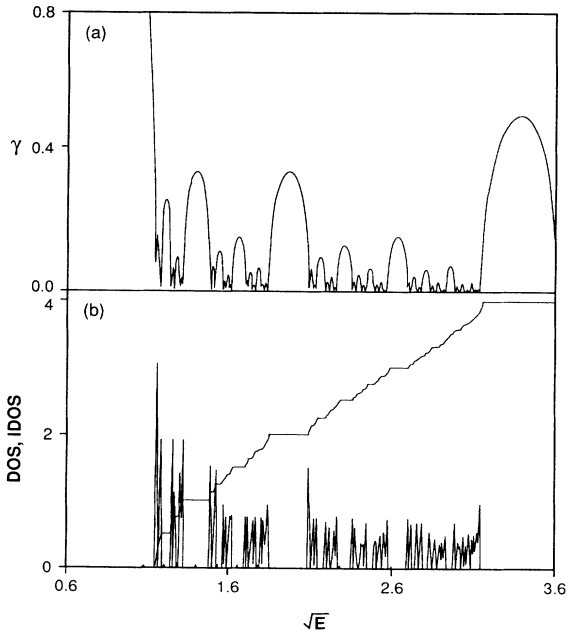

FIG. 1. Energy dependence of (a) γ and (b) DOS and integrated DOS for $N=2^{11}-1=2047$, $R=1.5$, and $F=0$. γ and DOS clearly show self-similarity.

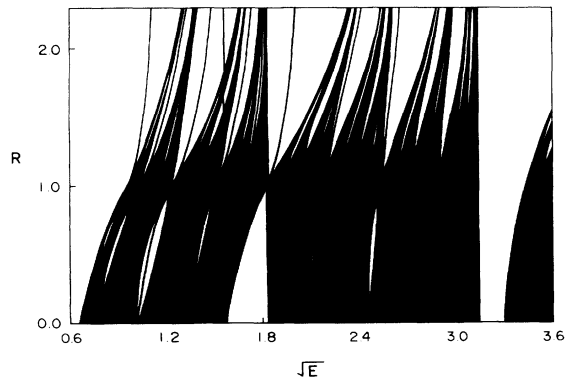

FIG. 2. R dependence of the DOS for a system with $N=2^8-1=255$ and $F=0$. Clustering of the eigenvalues for $R>1$ has different behavior from that for $R<1$.

one that has zero Lebesgue measure. Meanwhile, the splitting in the regime $0<R<1$ is less clear. Only the gaps due to lower levels are appreciable, and those of higher levels are negligible. In this case the spectrum in the infinite-system-size limit will form a fractal with positive Lebesgue measure,[11] which seems to be related with "recurrent" absolute continuous spectrum called by Avron and Simon[16] that is found in the Cantor set of positive Lebesgue measure. The physical significance of this classification of continuous spectra comes from the connection between the transport properties and the nature of the spectrum. The usual "purely" absolutely continuous spectrum has good transport properties, and the singular continuous spectrum has bad transport properties. The recurrent absolute continuous spectrum has intermediate transport properties between them. An illustration of this is shown in Fig. 3. Note that the states appearing in the gap regions are due to the finite size of the system. These gap states will disappear as the size of the system increases.

When the electric field is applied, degeneracies due to equivalent potentials begin to be lifted, resulting in additional eigenstates. Figure 4 shows (a) γ and (b) the DOS for the same parameters as in Fig. 1, except that $F=5.0\times10^{-5}$. Some eigenstates move into the gap regions, and the narrow subgaps that occurred in Fig. 1 disappear [see Fig. 4(a)]. The inset of Fig. 4(b) shows the DOS for incident momentum $k_{\text{in}}=E^{1/2}=1.515-1.620$, which forms ladderlike structure with nonuniform spacings. As the field increases, some eigenstates will move into the gaps more deeply, and the DOS will distribute broadly for large fields, resulting in a continuous spectrum, as in the cases of periodic and disordered systems. To understand the behavior of the field-induced states, we study the transmission coefficient introduced in the next section.

B. Transmission coefficients

The electronic states of a system under consideration can be classified by the quantity $\xi\equiv N\gamma=-\ln T$, where T is the transmission coefficient of an incident electron. For extended states, ξ shows a rapidly converging behavior with increasing length, and for exponentially localized states, ξ shows a linearly increasing behavior. Meanwhile, ξ for critical states displays an oscillatory be-

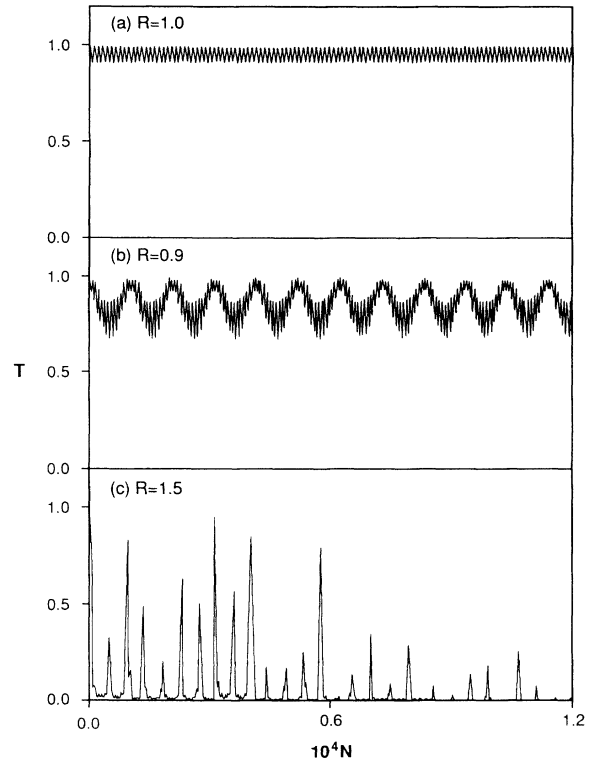

FIG. 3. N dependence of transmission coefficient T for $N=12\,000$ and (a) $R=1.0$, (b) $R=0.9$, (c) $R=1.5$.

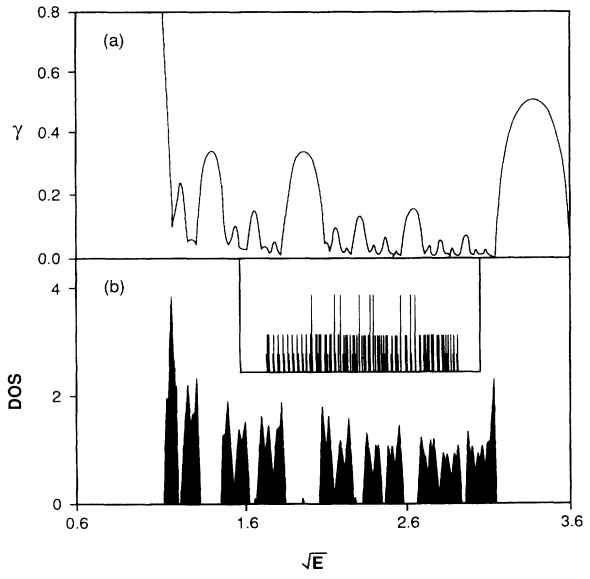

FIG. 4. (a) γ and (b) DOS for parameters as in Fig. 1 but for $F=5.0\times10^{-5}$. The inset for $k_{\text{in}}=1.515-1.620$ shows nonuniform ladderlike structure.

havior. One can calculate T and ξ in the following way:[17] From Eq. (3), one can write

$$\begin{bmatrix}\Psi_{N+1}\\ \Psi_N\end{bmatrix}=\mathbf{P}^{(N)}\begin{bmatrix}\Psi_N\\ \Psi_{N-1}\end{bmatrix}=\mathbf{P}_N\begin{bmatrix}\Psi_1\\ \Psi_0\end{bmatrix} . \tag{6}$$

Here $\mathbf{P}^{(N)}$ is the promotion matrix for the Nth potential barrier, and $\mathbf{P}_N$ is the promotion matrix for the whole system, which is given by

$$\mathbf{P}^{(N)}=\begin{bmatrix}E_N/X_N & -X_{N-1}/X_N\\ 1 & 0\end{bmatrix} \tag{7}$$

and

$$\mathbf{P}_N=\mathbf{P}^{(N)}\mathbf{P}_{N-1}=\prod_{n=1}^{N}\mathbf{P}^{(N-n+1)} . \tag{8}$$

From these equations and the plane-wave solutions in each cell, T is given by

$$T=\frac{k_N}{k_{\rm in}}|t|^2=\frac{k_{\rm in}}{k_N|M_N^{11}|^2} , \tag{9}$$

where t is the transmission amplitude and M_N^{11} is the (1,1) component of the transfer matrix given by

$$\begin{aligned}|M_N^{11}|^2=\frac{1}{4\sin^2(k_N)}\{&(P_N^{11}+P_N^{12}+P_N^{21}+P_N^{22})^2+2(P_N^{11}P_N^{12}+P_N^{21}P_N^{22})[\cos(k_{\rm in})-1]\\ &-2(P_N^{11}P_N^{21}+P_N^{12}P_N^{22})[\cos(k_N)+1]-2P_N^{11}P_N^{22}[\cos(k_N+k_{\rm in})+1]\\ &-2P_N^{12}P_N^{21}[\cos(k_N-k_{\rm in})+1]\} .\end{aligned} \tag{10}$$

From Eq. (8), the recursion relations of the promotion matrices are given by

$$\begin{aligned}&P_N^{21}=P_{N-1}^{11},\quad P_N^{11}=\frac{E_N}{X_N}P_{N-1}^{11}-\frac{X_{N-1}}{X_N}P_{N-2}^{11} ,\\ &P_N^{22}=P_{N-1}^{12},\quad P_N^{12}=\frac{E_N}{X_N}P_{N-1}^{12}-\frac{X_{N-1}}{X_N}P_{N-2}^{12} .\end{aligned} \tag{11}$$

Thus one can calculate M_N^{11}, and ultimately T, by iterated applications of Eqs. (10) and (11).

Figure 5(a) shows the N dependence of the average values of ξ with respect to the length defined by $\bar{\xi}=-(1/N)\sum_{i=1}^{N}(\ln T_i)$ for a system of size $N=60\,000$ under an applied field $F=0$. The solid line represents the case that has potential parameter $R=0.9$, and the dashed line represents that of $R=1.2$. The incident energies are $E=7.300\,804\,000$ for $R=0.9$, and $E=6.291\,854\,839$ for $R=1.2$, respectively. For the $R=0.9$ case, the potential strength ranges from $(0.9)^{15}=0.205\,981\ldots$ to 1.0, and the potentials of higher levels can be regarded as perturbative quantities. Thus $\bar{\xi}$ is expected to show a behavior similar to that of a periodic system; the solid line in the figure shows the expected behavior, except for some fluctuations. For the $R=1.2$ case, the potential ranges from 1.0 to $(1.2)^{15}=15.407\,021\ldots$, and the structure is quite different from that of a periodic system. The behavior of $\bar{\xi}$ reveals this fact; it displays large fluctuations with various coupled oscillations. This behavior is consistent with the highly concentrated spectra given in Fig. 2. Although the self-similarity is not exactly shown, the coupled oscillations are presumably connected with it.

When the electric field is applied, the behavior of $\bar{\xi}$ changes considerably. Define F_0 to be the field strength at which the electric potential $Fx_n\sim F\times 2^{k_{\max}}$ is equal to the highest hierarchical potential V_n as follows:

$$F_0=U_0\left[\frac{R}{2}\right]^{k_{\max}} , \quad k_{\max}\gg 1 , \tag{12}$$

where $k_{\max}$ is the highest level of hierarchy of the system. Consider first the case $R<2$. If the applied field F is much larger than F_0, the incident electron gains electric energy that dominates over the hierarchical potential. The tunneling between gaps then becomes easier and $\bar{\xi}$ is expected to show extended behavior. On the other hand, if the applied field F is not larger than F_0, then there are so many hierarchical potentials that can dominate over the electric potential that the transport of an incident electron may become worse. Thus $\bar{\xi}$ is expected to show a localized behavior. However, this expectation is valid only for a finite system. When the size of the system goes to infinity, F_0 goes to zero and $\bar{\xi}$ is expected to show an extended behavior for arbitrary values of F. The numerically calculated $\bar{\xi}$ is given in Figs. 5(b) and 5(c). Figure 5(b) shows the N dependence of $\bar{\xi}$ as the applied electric field changes from 0.005 to 0.150. The values of $\bar{\xi}$ increase monotonically, forming logarithmiclike functions, except for some cusps. The cusps appearing in the figure reveal Zener tunneling through the main gaps, and the positions of the cusps correspond to the positions at which the incident electron begins to leave a band and tunnel the gap. To determine the extent of localization, we plot the $\ln N$ dependence in the inset. From this figure one can see $T\sim N^{-\beta}$, where $\beta\sim O(1/F)$; i.e., the transmission coefficient shows a power-law localized behavior. Note that the power-law localized behavior of T also appears in disordered systems in the presence of an electric field,[5] and that this behavior is characteristic of the finite size of the system, as previously mentioned. Figure 5(c) shows $\bar{\xi}$ for $F\gg F_0$. The solid line exhibits an extended behavior, as expected. From this we know that in the finite system the transition from critical states ($F=0$) to extended states has occurred, although we could not determine the critical field at which the transition occurred. One noteworthy point is that we have observed some coupled oscillatory behavior of $\bar{\xi}$ that is unlike that of ordinary extended states. This may be a property particular to the field-induced extended states,

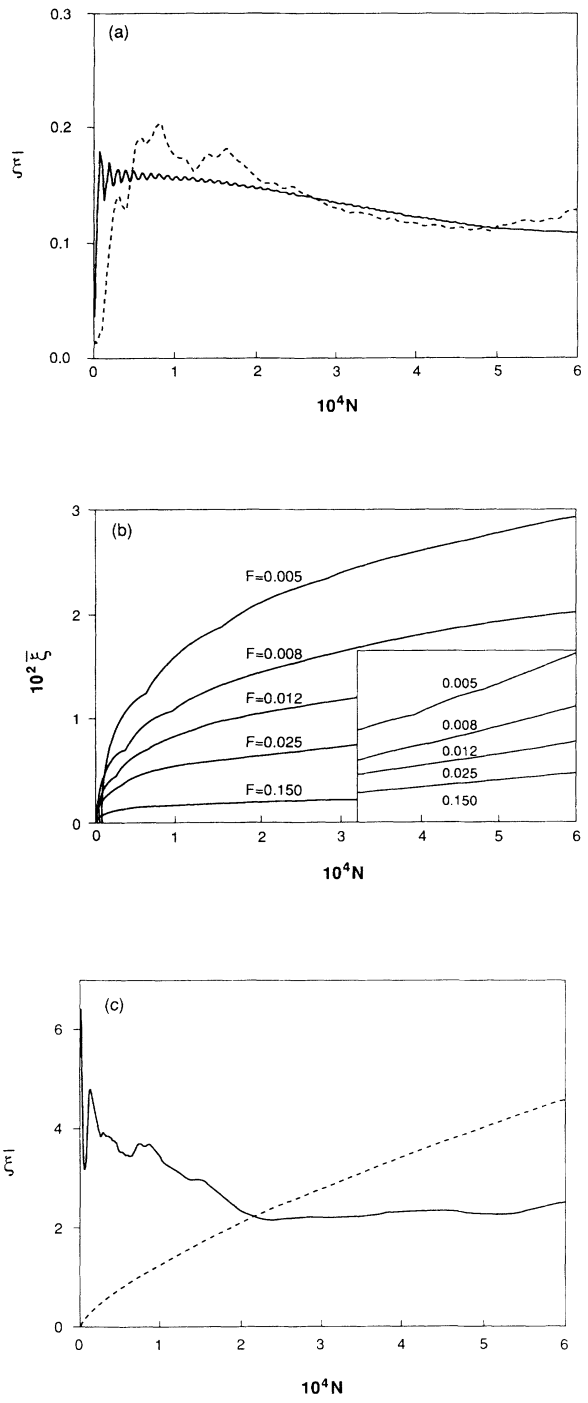

FIG. 5. (a) N dependence of $\bar{\xi}$ for $R=1.2$, $E=6.291\,854\,839$ (dashed line), and $R=0.9$, $E=7.300\,800\,400$ (solid line). $N=60\,000$ and $F=0$. The real value of $\bar{\xi}$ for $R=1.2$ is three times as large as that for $R=0.9$. (b) N dependence of $\bar{\xi}$ under $F=0.005$–0.150 ($R=1.2$). The inset represents $\ln N$ dependence, and it shows a power-law decay of the transmission coefficients. The horizontal axis of the inset ranges from 9.239 607 to 11.090 125. (c) N dependence of $\bar{\xi}$ for large fields. The solid line represents a state for $R<2$ and exhibits an extended behavior. The dashed line represents a state for $R>2$ and exhibits a power-law localized behavior. The real value of $\bar{\xi}$ for $R>2$ is 10^4 times as large as that for $R<2$.

and we investigate the property further by the method of multifractal analysis that is presented in the next section.

For the $R>2$ case, F can exceed F_0 in the finite system, and $\bar{\xi}$ can then be shown to have an extended behavior. However, in the infinite-system-size limit, F_0 goes to infinity, which means that the hierarchical potential always dominates over the electric potential. So the transport of the incident electron becomes very poor, and we expect $\bar{\xi}$ to show a localized behavior for arbitrary values of F. A typical behavior is shown in Fig. 5(c), which is similar to that of Fig. 5(b). Thus we believe that the field-induced states for $R>2$ are power-law localized states. The multifractal analysis for the wave functions belonging to this state is given in the next section.

C. Multifractal analysis

From the study of the transmission coefficients, we know that applied electric fields change a critical state to an extended state for $R<2$ and to power-law localized state for $R>2$. We also know that the behavior of $\bar{\xi}$ for field-induced extended states has features different from those of ordinary extended states. In connection with this fact, it is interesting to note that, as previously mentioned, Delyon *et al.*[6] proved the existence of a transition from power-law localized to extended states in a disordered system as the field strength increases, but could not determine whether the spectrum of extended states is singular continuous or absolute continuous. Furthermore, Kim and Socolar,[18] who studied the effects of an electric field on a quasiperiodic system with a Fibonaccian sequence of potentials, found that almost all states are changed from critical to extended states with increasing field strength, while some states still remain critical and coexist with most extended states. With this background, we performed a multifractal analysis[19] on the wave functions of the field-induced states, which is known to be an effective method in distinguishing different types of wave functions.

The wave functions used in the analysis are obtained by the inverse iteration method.[20] The probability measure $p_i(l)$ of finding the electron within the ith segment is given by

$$p_i(l)=\frac{\sum_{j=(i-1)l+1}^{il}|\Psi_j|^2}{\sum_{k=1}^{N}|\Psi_k|^2}, \quad i=1,2,\ldots,N/l\ , \tag{13}$$

where the length of the system N is assumed to be divided into N/l segments, each of length l. Given $p_i(l)$, the partition function (or generalized moment) $Z(q,l)$ is defined as

$$Z(q,l)=\sum_{i=1}^{N/l}[p_i(l)]^q\ . \tag{14}$$

Assuming $Z(q,l)$ behaves as a power of l, $Z(q,l)\sim l^{\tau(q)}$, the exponent $\tau(q)$ can be determined from the plots of $\ln Z(q,l)$ versus $\ln l$.

Figure 6(a) represents $\ln Z(q,l)$ versus $\ln l$ for a wave function belonging to a field-induced extended state, which is obtained when $R=0.9$, $E=7.300\,800\,400$, $N=2^{14}-1=16\,383$, and $F=6.80$. For a given q, the

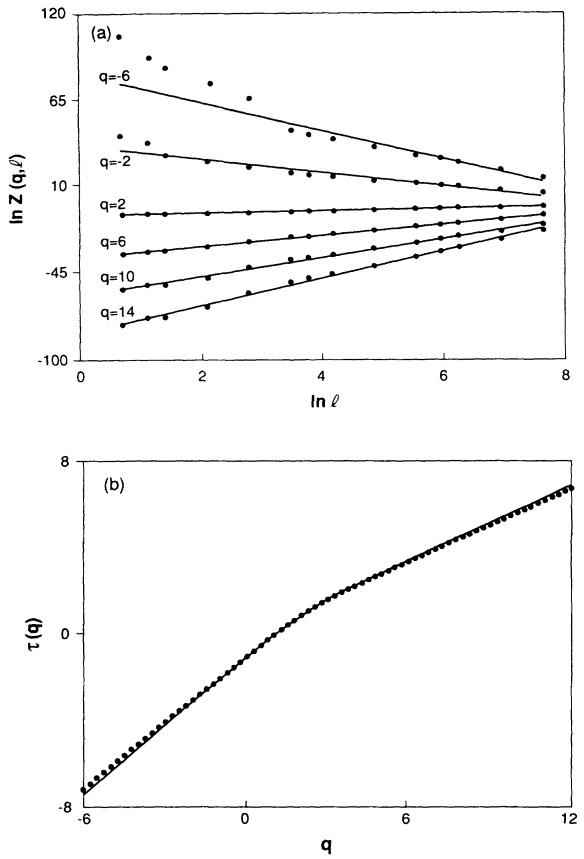

FIG. 6. (a) Plots of $\ln Z(q,l)$ vs $\ln l$ for $q=-6$, -2, 2, 4, 10, and 14 on the field-induced extended state with $R=0.9$, $E=7.300\,800\,400$, $N=16\,383$, and $F=6.80$. (b) Plot of $\tau(q)$ vs q. The dotted curve is obtained from the slopes in (a), while the solid line is obtained directly from $Z(q,l)\sim l^{\tau(q)}$ for a fixed value of l.

slope of the straight line gives $\tau(q)$. We use the least-squares method to fit a straight line and obtain $\tau(q)$, which is given in Fig. 6(b). For positive and small negative values of q, the fluctuations of the curves are small, and thus the fitting of a straight line is easy. However, for large negative values of q, there exist large fluctuations that make it very difficult to fit a straight line to it. The fluctuations seem to be related to the fact that the assumption that the partition function is a power of l may not always be correct, and thus the normal multifractal behavior breaks down at some negative value of q.[21] So we consider only positive and small negative values of q for which the fitting of a straight line to obtain $\tau(q)$ is reasonable. Note that similar fluctuations have previously been found in the analysis of an incommensurate system,[22] and therein the straight line has been obtained by regarding the fluctuations as oscillations around a straight line. For a simple fractal or nonfractal case, one obtains a straight line $\tau(q)=D_0(q-1)$, where D_0 is the Hausdorff dimension, and $D_0=1$ for a nonfractal case. Thus the existence of a nonlinear $\tau(q)$ indicates a multifractal behavior. The dotted curve in Fig. 6(b) that is obtained from the slopes of the straight lines in Fig. 6(a) shows a nonlinear function of q, which means that the wave function belonging to the field-induced extended state has multifractal behavior. The solid line in the figure represents the result obtained directly from $Z(q,l)\sim l^{\tau(q)}$ with a fixed value of l, which is the instantaneous slope of $\ln Z(q,l)$ versus $\ln l$ at a given l. The solid line has almost the same behavior as the dotted line except in the range of large negative q, where the instantaneous slope is different from the average slope owing to the large fluctuations. In connection with this fact, it is interesting to note that Severin and Riklund[23] argued that $\tau(q,l)$ shows multifractality up to all length scales for critical states, while it shows a fractal-nonfractal crossover at a certain critical length scale l_c for extended states. They found that the wave functions belonging to the spectrum with finite measure have a finite critical length l_c, while the states belonging to the spectrum with zero measure do not. Thus it can be used as a criterion to decide whether or not a state has multifractality for a given l, although the (f,α) curves obtained from each $\tau(q)$ have slightly different values for large negative values of q. We calculated $\tau(q,l)$ of the field-induced extended states for various values of l, and obtained a nonlinearity up to $l\sim 2000$, which is one-eighth of the size of the system. This means that the field-induced extended states either have an l_c greater than 2000 or have no l_c where the crossover to multifractality occurs. On the basis of this fact, the spectrum in the presence of large fields is expected to be a singular continuous or recurrent absolute continuous one.

Making the scaling ansatz $p_i(l)\sim l^{\alpha_i(q)}$ and assuming the density of scaling exponents to be $\Omega(\alpha)d\alpha \sim l^{-f(\alpha)}d\alpha$, one can obtain the multifractal spectrum (f,α) using the relations

$$f(\alpha)=q\alpha-\tau(q),\quad \alpha(q)=\frac{d\tau(q)}{dq}\ . \tag{15}$$

As is well known, the extended wave function has $f=\alpha=1$, and the localized wave function has an $f(\alpha)$ consisting of two points, $f(\alpha=0)=0$ and $f(\alpha=\infty)=1$. The point $\alpha=0$ corresponds to the sites with nonzero Ψ_i, and $\alpha=\infty$ to all other sites. For a critical wave function, $f(\alpha)$ has a smooth curve defined on the finite interval $[\alpha_{\min},\alpha_{\max}]$.

Figure 7(a) shows the (f,α) curve for a field-induced extended state with the same parameters as in Fig. 6(a), and $l\sim 2000$. As previously mentioned, the fitting of a straight line to obtain $\tau(q)$ for large negative values of q is so difficult that we consider only the curve corresponding to positive values and small negative values of q. Just considering the part corresponding to these values of q, we can see a smooth curve that indicates the multifractal behavior. The same behavior is observed for a wave function with $R=1.2$, $E=6.291\,854\,839$, $F=13.00$, and $l\sim 2000$ [see Fig. 7(b)]. We also performed the same analysis by varying l and obtained smooth (f,α) curves indicating multifractality, which is consistent with the result obtained in the analysis of $\tau(q)$. Note that the Hausdorff fractal dimension $f(q=0)=D_0=1$, because the support for the measure remains the original line segment at any stage, which always holds in the analysis of wave functions.

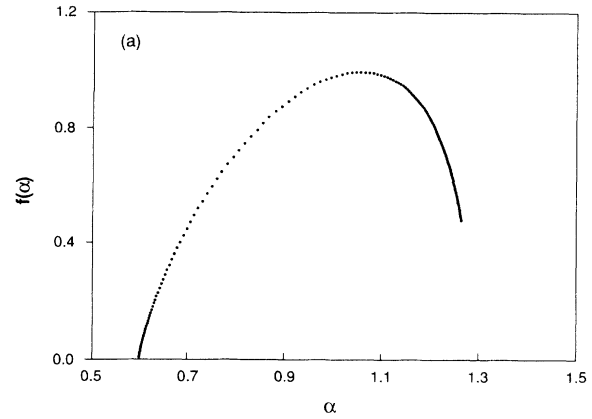

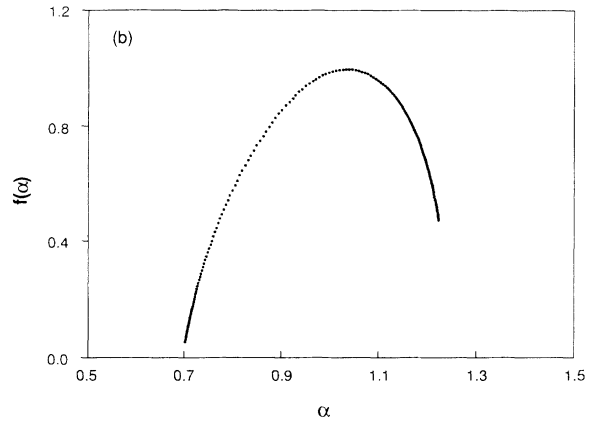

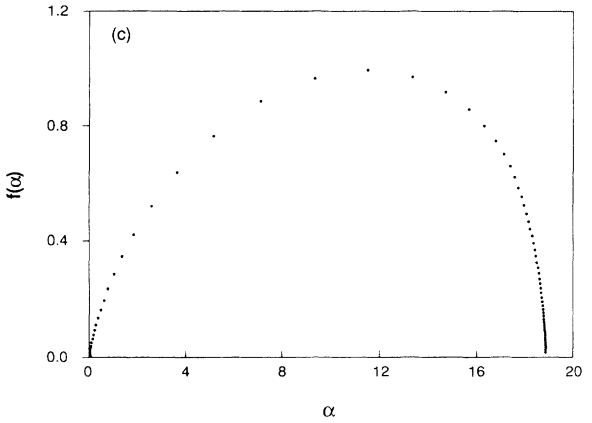

FIG. 7. (a) (f,α) spectrum for the wave function belonging to an extended state with $R=0.9$, $F=6.80$, and $E=7.300\,800\,400$. (b) (f,α) spectrum for the wave function belonging to an extended state with $R=1.2$, $F=13.00$, and $E=6.291\,854\,839$. (c) (f,α) spectrum for the wave function belonging to a power-law localized state with $R=2.2$, $E=6.300\,100\,000$, and $F=32.00$.

Figure 7(c) shows the (f,α) curve for a wave function belonging to the power-law localized state. The parameters are $R=2.2$, $E=6.300\,100\,000$, $F=32$, and $l\sim2000$. For small values of l, we obtained a smooth curve. However, for large values of l, the (f,α) spectrum concentrates around point $f=\alpha=0$ for large values of q, and gives very large values of α as q goes to zero. Note that the smooth curve in the figure is due to the finite size of the system. In the infinite-system-size limit, the spectrum is expected to go to the two points $f(\alpha=0)=0$ and $f(\alpha=\infty)=1$. This is a feature of the (f,α) curve particular to the localized state. Recently, Mato and Caro,[24] who studied a one-dimensional disordered system with an electric field, argued that the wave function belonging to the power-law localized state has no multifractal character, which is consistent with our result for the power-law localized state for large values of l.

We believe that the multifractality obtained in the wave functions of the field-induced states is not due to the hierarchical character of the system, but rather is due to the effect of the applied field. The periodic or incommensurate systems have no parameters such as R in a hierarchical system with which to determine whether the field-induced states are power-law localized or extended states. The behavior of $\bar{\xi}$ in periodic or incommensurate systems exhibits extended behavior under large electric fields. We have performed a multifractal analysis on these states,[25] and obtained results similar to those for the hierarchical system with $R<2$. It is therefore a possibility that the multifractality is related to the electric field rather than the potential structure of the system.

III. SUMMARY

In this paper we have studied numerically the effect of an applied electric field on a one-dimensional hierarchical system. As the field increases, the DOS becomes broad and eventually goes to a continuum. The properties of the states belonging to these spectra can be well described by a quantity $\bar{\xi}$. The behavior of $\bar{\xi}$ depends on the parameter R. In the $R>2$ case, it shows a power-law localized behavior for arbitrary values of the applied field. On the other hand, in the $R<2$ case, it shows a power-law localized behavior for small fields and extended behavior for large fields. However, the occurrence of the power-law localized behavior in the $R<2$ case may be the effect of finite system size, and we believe, based on Eq. (12), that in the infinite-system-size limit it will show an extended behavior.

We have performed a multifractal analysis on the wave functions of the field-induced states. In the $R<2$ case, the field-induced extended states show a multifractal behavior up to $l\sim2000$, which means that l_c is equal to or greater than 2000 and that the states are not ordinary extended states. It is therefore quite possible that the spectra are not purely absolute continuous ones, but rather are singular continuous or recurrent absolute continuous ones. In the $R>2$ case, the power-law localized states

show multifractality only for small values of l, which is consistent with previous results. In this study, we took the potentials to be of the δ-function type. It would be interesting to know whether or not more realistic systems with potentials, such as ones of a square-barrier type, show the same behavior. These results will be reported soon.

ACKNOWLEDGMENTS

This work was supported in part by the Scientific Research Center through the Center for Theoretical Physics in Seoul National University. We would like to thank Y. J. Kim for helpful discussions on the electronic properties of the system.

[1]G. H. Wannier, Phys. Rev. **117**, 432 (1960); S. Nagai and J. Kondo, J. Phys. Soc. Jpn. **49**, 1255 (1980); E. Cota, J. V. José, and G. Monsiváis, Phys. Rev. B **35**, 8929 (1987).

[2]D. Emin and C. F. Hart, Phys. Rev. B **36**, 7353 (1987).

[3]J. Bleuse, G. Bastard, and P. Voisin, Phys. Rev. Lett. **60**, 220 (1988); E. E. Mendez, F. Agulló-Rueda, and J. M. Hong, *ibid.* **60**, 2426 (1988).

[4]J. E. Avron, J. Zak, A. Grossman, and L. Gunther, J. Math. Phys. **18**, 918 (1977); F. Bentosela, R. Carmona, P. Duclos, B. Simon, B. Souillard, and R. Weder, Commun. Math. Phys. **88**, 387 (1980).

[5]C. M. Soukoulis, J. V. José, E. N. Economou, and Ping Sheng, Phys. Rev. Lett. **50**, 764 (1983); E. Cota, A. Caro, and A. López, Phys. Rev. **36**, 3002 (1985); C. Schwartz and C. S. Ting, *ibid.* **36**, 7169 (1987); J. Leo and B. Movaghar, *ibid.* **38**, 8061 (1988).

[6]F. Delyon, B. Simon, and B. Souillard, Phys. Rev. Lett. **52**, 2187 (1984); see also V. N. Prigodin, Zh. Eksp. Teor. Fiz. **79**, 2338 (1980) [Sov. Phys. JETP **52**, 1185 (1980)]; T. R. Kirkpatrick, Phys. Rev. B **33**, 780 (1986).

[7]J. V. José, G. Monsiváis, and J. Flores, Phys. Rev. B **31**, 6906 (1985); F. Bentosela, V. Grecchi, and F. Zironi, *ibid.* **31**, 6909 (1985).

[8]M. Kohmoto, L. P. Kadanoff, and C. Tang, Phys. Rev. Lett. **50**, 1870 (1983); S. Ostrund, R. Pandit, D. Rand, H. J. Schellnhuber, and E. D. Siggia, *ibid.* **50**, 1873 (1983); M. Kohmoto, B. Sutherland, and C. Tang, Phys. Rev. B **35**, 1020 (1987).

[9]S. Aubry and G. André, Ann. Isr. Phys. Soc. **3**, 133 (1980); B. Simon, Adv. Appl. Math. **3**, 463 (1982); J. B. Sokoloff, Phys. Rep. **126**, 189 (1985); C. M. Soukoulis and E. N. Economou, Phys. Rev. Lett. **48**, 1043 (1982); M. Johansson and R. Riklund, Phys. Rev. B **42**, 8244 (1990).

[10]G. Gumbs and M. K. Ali, Phys. Rev. Lett. **60**, 1081 (1988); J. Q. You and Q. B. Yang, J. Phys. Condens. Matter **2**, 2093 (1990).

[11]D. Würtz, T. Schneider, A. Politi, and M. Zannetti, Phys. Rev. B **39**, 7829 (1989).

[12]R. Livi, A. Maritan, and S. Ruffo, J. Stat. Phys. **52**, 595 (1988).

[13]H. A. Ceccatto, W. P. Keirstead, and B. A. Huberman, Phys. Rev. A **36**, 5509 (1987); H. A. Ceccatto and W. P. Keirstead, J. Phys. A **21**, L75 (1987).

[14]H. E. Roman, Phys. Rev. B **36**, 7173 (1987); **37**, 1399 (1988).

[15]P. Dean, Rev. Mod. Phys. **44**, 127 (1972).

[16]J. E. Avron and B. Simon, J. Funct. Anal. **43**, 1 (1981); J. E. Avron and B. Simon, Commun. Math. Phys. **82**, 101 (1981).

[17]A. D. Stone, J. D. Joannopoulos, and D. J. Chadi, Phys. Rev. B **24**, 5583 (1981).

[18]Y. J. Kim and J. E. S. Socolar (unpublished).

[19]H. Halsey, M. H. Jensen, L. P. Kadanoff, I. Procaccia, and B. I. Shraiman, Phys. Rev. A **33**, 1141 (1986).

[20]E. Roman and C. Wiecko, Z. Phys. B **62**, 163 (1986).

[21]N. Gupte and R. E. Amritkar, Phys. Rev. A **39**, 5466 (1989); R. Blumenfeld and A. Aharony, Phys. Rev. Lett. **62**, 2977 (1989).

[22]M. Johansson and R. Riklund, Phys. Rev. B **42**, 8244 (1990).

[23]M. Severin and R. Riklund, Phys. Rev. B **39**, 10 362 (1989).

[24]G. Mato and A. Caro, J. Phys. Condens. Matter **1**, 901 (1989).

[25]C. S. Ryu, G. Y. Oh, and M. H. Lee (unpublished).